

A new Greenland ice core chronology for the last glacial termination

S. O. Rasmussen¹, K. K. Andersen¹, A. M. Svensson¹, J. P. Steffensen¹, B. M. Vinther¹, H. B. Clausen¹, M.-L. Siggaard-Andersen^{1,2}, S. J. Johnsen¹, L. B. Larsen¹, D. Dahl-Jensen¹, M. Bigler^{1,3}, R. Röthlisberger^{3,4}, H. Fischer², K. Goto-Azuma⁵, M. E. Hansson⁶, and U. Ruth²

Abstract. We present a new common stratigraphic time scale for the NGRIP and GRIP ice cores. The time scale covers the period 7.9–14.8 ka before present, and includes the Bølling, Allerød, Younger Dryas, and Early Holocene periods. We use a combination of new and previously published data, the most prominent being new high resolution Continuous Flow Analysis (CFA) impurity records from the NGRIP ice core. Several investigators have identified and counted annual layers using a multi-parameter approach, and the maximum counting error is estimated to be up to 2% in the Holocene part and about 3% for the older parts. These counting error estimates reflect the number of annual layers that were hard to interpret, but not a possible bias in the set of rules used for annual layer identification. As the GRIP and NGRIP ice cores are not optimal for annual layer counting in the middle and late Holocene, the time scale is tied to a prominent volcanic event inside the 8.2 ka cold event, recently dated in the DYE-3 ice core to 8236 years before A.D. 2000 (b2k) with a maximum counting error of 47 years. The new time scale dates the Younger Dryas – Preboreal transition to 11,703 b2k, which is 100–150 years older than according to the present GRIP and NGRIP time scales. The age of the transition matches the GISP2 time scale within a few years, but viewed over the entire 7.9–14.8 ka section, there are significant differences between the new time scale and the GISP2 time scale. The transition from the glacial into the Bølling interstadial is dated to 14,692 b2k. The presented time scale is a part of a new Greenland ice core chronology common to the DYE-3, GRIP and NGRIP ice cores, named the Greenland Ice Core Chronology 2005 (GICC05). The annual layer thicknesses are observed to be log-normally distributed with good approximation, and compared to the Early Holocene, the mean accumulation rates in the Younger Dryas and Bølling periods are found to be $47 \pm 2\%$ and $88 \pm 2\%$, respectively.

PREPRINT. Accepted for publication in Journal of Geophysical Research (28 Nov. 2005). Copyright 2005 American Geophysical Union. Further reproduction or electronic distribution is not permitted.

1. Introduction

A wealth of information about palaeoclimate can be extracted from polar ice cores, but the full potential of these data can be exploited only with a reliable depth–age relation. Especially when studying the dramatic climatic transitions of the past, accurate age estimates are of great importance because the relative timing of climate changes around

the globe gives indications of the causes and mechanisms for rapid climatic changes [Bond et al., 1993; Blunier et al., 1998]. Much effort has therefore been put into developing time scales for ice cores, based either on identification and counting of annual layers or modeling the depth–age relationship [Hammer et al., 1978; Hammer, 1989]. Greenland ice cores can be dated by annual layer counting when the accumulation rate is sufficient to resolve annual layers, and the time scales of different ice cores can be matched and validated using volcanic layers and other independently dated stratigraphic markers [Clausen et al., 1997; Anklin et al., 1998]. The DYE-3 and GRIP ice cores were dated about 8 ka back by counting annual layers in the stable isotope and electrical conductivity measurement profiles [Hammer et al., 1986; Hammer, 1989; Johnsen et al., 1992]. Below this, annual layers were identified using GRIP chemistry data as well. In the glacial part of GRIP, discontinuous annual layer counting was used as input for ice flow modeling [Dansgaard et al. 1993; Johnsen et al. 1995 (ss09 time scale); Johnsen et al., 2001 (ss09sea time scale)], while the GISP2 ice core was dated using stratigraphic methods also in the glacial, relying primarily on the visual layers in the ice [Alley et al., 1997; Meese et al., 1997]. As discussed by Southon [2004], the different time scales of GRIP and GISP2 are up to several thousand years offset in parts of the glacial, and there

¹Ice and Climate, Niels Bohr Institute, University of Copenhagen, Denmark

²Alfred-Wegener-Institute for Polar and Marine Research, Bremerhaven, Germany

³Climate and Environmental Physics, Physics Institute, University of Bern, Switzerland

⁴Now at British Antarctic Survey, Cambridge, UK

⁵National Institute of Polar Research, Tokyo, Japan

⁶Department of Physical Geography and Quaternary Geology, Stockholm University, Sweden

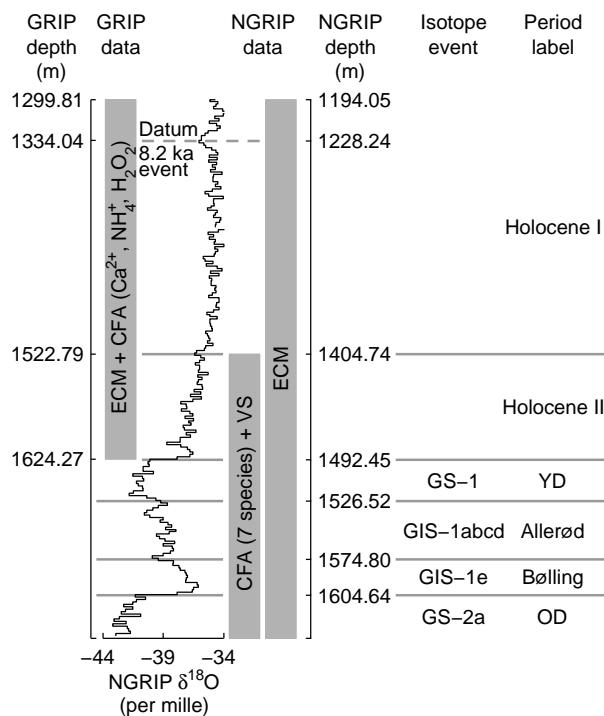


Figure 1. Overview of the data series used for the different parts of the GRIP and NGRIP ice cores. VS refers to the visual stratigraphy data, ECM are electrical conductivity measurement data. The period labels are the names used throughout this work to identify the different time periods. YD and OD refer to the Younger Dryas and Oldest Dryas, respectively. The isotope event names refer to those of Björck et al. [1998].

are significant differences in the Holocene as well.

Drilling of the NGRIP ice core was completed successfully in 2003 [Dahl-Jensen et al., 2002; NGRIP members, 2004]. Liquid water was found when the drill penetrated the ice sheet, revealing melting point temperatures at the bedrock. The melting at the base limits the age of the ice in the NGRIP ice core to be approx. 123 ky old [NGRIP members, 2004]. The combination of moderate accumulation rates (19 cm of ice equivalent per year in present time) and bottom melting result in a different flow pattern than that of GRIP and GISP2, and the annual layers are thus more than 5 mm thick over the entire length of the NGRIP core. This means that in the middle and early part of the glacial the annual layers are thicker than those observed in the GRIP and GISP2 ice cores [NGRIP members, 2004; Dahl-Jensen et al., 1993; Johnsen et al., 2001; Meese et al., 1997]. This fact, and the development of new high resolution impurity measurement techniques, makes the NGRIP ice core ideal for stratigraphic dating purposes, and has motivated the initiation of the Copenhagen Ice Core Dating Initiative, with the construction of a new stratigraphic timescale for the GRIP and NGRIP ice cores as one of the main objectives. Here we present a stratigraphic time scale for the period 7.9–14.8 ka before A.D. 2000 (b2k), using multi-parameter data from both the GRIP and NGRIP ice cores. The datum of the presented time scale is a readily recognizable volcanic event inside the characteristic 8.2 ka cold event, dated using data from the DYE-3 ice core. In the section 7.9–10.3 ka before present, the time scale is based on new annual layer counting using existing impurity records from the GRIP ice core [Führer et al., 1993; 1996; 1999]. From 10.3 ka b2k and back

also NGRIP impurity records are available, and down to the Younger Dryas – Preboreal transition (henceforth named the YDPB transition) the time scale is based on the combined GRIP-NGRIP data set. For NGRIP, the time scale continues through the Younger Dryas, Allerød and Bølling periods back to 14.8 ka before present. The new time scale is named the Greenland Ice Core Chronology 2005, or GICC05.

In order to be able to refer to the different sections of the presented time scale in a short and unambiguous way, the names Holocene I, Holocene II, Younger Dryas, Allerød, Bølling, and Oldest Dryas are used as illustrated in Figure 1, although this use does not comply with the formal bio-stratigraphic definitions of the periods. The transition depths used to define the onset and end of the Bølling and Younger Dryas periods are derived from deuterium excess data (the deuterium excess is defined as $\delta D - 8\delta^{18}O$). In each of these transitions, the deuterium excess changes abruptly, and the change occurs prior to, or simultaneously with, changes in all other climate proxies. As changes in the deuterium excess are connected to changes in the moisture sources [Jouzel and Merlivat, 1984; Johnsen et al., 1989; Taylor et al., 1997; Masson-Delmotte et al., 2005a; 2005b], the abrupt shifts in deuterium excess indicate that dramatic reorganizations of the atmospheric circulation took place at the onset of these transitions, followed by more gradual changes in temperature and ice core impurity content. A discussion of the implications of these observations is beyond the scope of this work, but it should be stressed that the timing of the transitions as defined by the deuterium excess must be expected to precede changes in e.g. temperature and vegetation recorded in other archives.

All ages in this work are reported in calendar years relative to the year A.D. 2000. Unfortunately the BP notation has in several instances been used with reference to other years than the conventional A.D. 1950 when reporting ice cores results. To avoid further confusion, and to underline the independency from e.g. radiocarbon-based dating, the notation b2k is introduced, being both short and unambiguous.

2. Data

For NGRIP, Continuous Flow Analysis (CFA) data of soluble ions were used for identification of annual layers [Bigler, 2004; Röthlisberger et al., 2000]. The resolution of the $[NH_4^+]$, $[Ca^{2+}]$, and conductivity series has been enhanced as described in Rasmussen et al. [2005], by correcting for the effect of dispersion in the CFA system using deconvolution techniques. The correction method uses the measured smooth response to a sudden concentration jump, obtained from calibration measurements, to estimate the mixing strength and restores as much as possible of the high-frequency part of the signal taking into account the presence of measurement noise. Moreover, CFA dust data (the number concentration of particles with diameter larger than $1.0\mu m$) of Ruth et al. [2003] were used. Electrical conductivity measurement (ECM) data representing the acidity of the ice were used [Dahl-Jensen et al., 2002]. All ECM profiles are shown as $[H^+]$ in $\mu equiv./kg$. The visual stratigraphy (VS) grey-scale refraction profile of Svensson et al. [2005] were also included, but as the raw VS data contain many close, thin layers representing sub-annual variations, we used a profile smoothed by applying a Gaussian filter with $s = 4$ mm.

The ice core drill got stuck in 1997 during the NGRIP drilling operation and a new core had to be drilled. The two cores are referred to as NGRIP1 and NGRIP2, respectively. Measurements have been performed on the NGRIP1 core down to a depth of 1372 m, while measurements on the NGRIP2 core start at a depth of 1346 m (corresponding to

Table 1. Data sets used in the construction of the presented time scale.

Ice core	Species	Depth Interval (m)	Sampling resolution (mm)	Estim. effective resolution ^a (mm)
NGRIP2	CFA: NH_4^+ , Ca^{2+} , Conductivity (resolution enhanced)	1404–1607	1	10 – 15 ^b
	CFA: NO_3^- , Na^+ , SO_4^{2-} , Dust	1404–1607	1	15 – 25 ^b
	Visual Stratigraphy	1404–1607	< 1	~ 3
	ECM	1346–1607	1	4
NGRIP1	ECM	1195–1372	10	40
GRIP	CFA: NH_4^+ , H_2O_2	1300–1624	2	~ 20 ^c
	CFA: Ca^{2+}	1300–1624	2	~ 50 ^c
	ECM	1300–1624	10	40

^a The effective resolution is the shortest wavelength that can be identified from the data.

^b The resolution varies with depth due to changing experimental conditions.

^c Approximate values obtained from inspection of the data. Fuhrer et al. [1993] report the resolution defined as the *e*-folding scale as 7, 12, and 35 mm for the NH_4^+ , H_2O_2 , and Ca^{2+} subsystems, respectively

approximately 9.5 ka b2k). In the zone of overlap the mean offset between NGRIP1 and NGRIP2 is 0.43 m, with the same feature appearing at greater depths in the NGRIP1 core than in the NGRIP2 core [Hvidberg et al., 2002]. All depths are NGRIP2 depths unless noted otherwise, and thus NGRIP1 data have been shifted 0.43 m to fit the NGRIP2 depth scale.

From the GRIP ice core, ECM data and the CFA records of $[\text{NH}_4^+]$, $[\text{H}_2\text{O}_2]$, and $[\text{Ca}^{2+}]$ obtained by Fuhrer et al. [1993; 1996; 1999] were used.

Table 1 lists the data series and the estimated effective resolution of each of the data series used. The effective resolution is defined for each series as the shortest cycle that can be identified in that series.

Model estimates of mean annual layer thicknesses in the NGRIP ice core [Johnsen et al., 2001; NGRIP members, 2004] are above 5 cm in the Holocene, around 3 cm in the Younger Dryas, about 4 cm in Bølling and Allerød, and 2–3 cm in the Oldest Dryas. The resolution of the CFA, ECM, and VS data thus allows identification of annual layers in the ice from the Holocene and back through the transition, while the resolution of the CFA data becomes marginal below the transition into the Bølling interstadial. Preliminary results show that the CFA data quality improves at greater depths, and it is thus possible to use CFA data for the identification of annual layers within most interstadials, where the accumulation is roughly twice that of the stadials. During the cold stadials annual layer identification has to rely mostly on VS and ECM.

3. Observed seasonality

Many of the impurity records obtained from Greenland ice cores exhibit annual variations [Beer et al., 1991; Whitlow et al., 1992; Fischer and Wagenbach, 1996]. The CFA, ECM, and VS data from GRIP and NGRIP are so highly resolved that the intra-annual timing of the different species is clearly detected at all depths. In the relatively warm periods (the Holocene, the Bølling and part of the Allerød period) the different species peak at different times of the year. The relative timing of the species resembles that observed for recent times [Whitlow et al., 1992; Laj et al., 1992; Steffensen, 1988; Anklin et al., 1998; Fuhrer et al., 1993; Bory et al., 2002]. A typical annual layer is characteristic by having the sea salt dominated $[\text{Na}^+]$ peaking in late winter. The VS record generally contains much more than one peak per year and is not easy to interpret, but in general there are layers of high refraction (cloudy bands) at spring-time, coinciding with high dust content, high $[\text{Ca}^{2+}]$ and dips in the $[\text{H}_2\text{O}_2]$ curve. Summer is characterized by high

concentration of $[\text{NH}_4^+]$, $[\text{NO}_3^-]$, and sometimes of $[\text{SO}_4^{2-}]$. In general, dips in the ECM correlate with peaks in $[\text{NH}_4^+]$ and $[\text{Ca}^{2+}]$, while the electrolytical conductivity (henceforth just called the conductivity) is related to the total content of ions present in the meltwater and thus contains several peaks per year due to the different seasonality of the individual species. In the colder periods, the differences in seasonality almost vanish and most series peak simultaneously, making the conductivity record useful for identification of annual layers. The $[\text{NH}_4^+]$ signal does not consistently show clear annual cycles in the cold periods. In the colder periods, the annual signal in VS becomes more prominent, but the VS record still contains more than one peak per year on average.

It should be noted that although there is an annual $[\text{H}_2\text{O}_2]$ signal present in recently formed snow, this signal has been erased by diffusion at the depths in question in this work. However, because $[\text{H}_2\text{O}_2]$ is only preserved in ice with low dust levels [Fuhrer et al., 1993], the dips in the $[\text{H}_2\text{O}_2]$ curve indicate high dust content. As the GRIP $[\text{H}_2\text{O}_2]$ measurements have significantly higher resolution than the corresponding $[\text{Ca}^{2+}]$ measurements, details obscured by the low resolution of the $[\text{Ca}^{2+}]$ resolution are often resolved by the $[\text{H}_2\text{O}_2]$ data.

4. Identification of Annual Layers

Identification and subsequent counting of annual layers in ice cores has been performed in various ways. The most direct, practically as well as conceptually, is to base the identification on a single parameter, which is known to exhibit annual cycles. Langway, Jr., [1967], used visible features to establish one of the first stratigraphic time scales for a Greenland ice core, ranging a few hundred years back, but most often $\delta^{18}\text{O}$ data are used where the accumulation rate is sufficiently high. The $\delta^{18}\text{O}$ parameter is the obvious choice because the close connection between $\delta^{18}\text{O}$ and temperature makes it highly probable that the observed cycles actually represent annual layers. Mainly using $\delta^{18}\text{O}$ measurements, a time scale for the last 8 ka was constructed by counting of annual layers in the DYE-3 ice core [Hammer et al., 1986]. Another prominent example of a single parameter stratigraphic time scale is that of the Byrd ice core, which was dated some 50,000 years back in time primarily using ECM data containing clear annual cycles [Hammer et al., 1994]. When more parallel data series with sufficient resolution are available from the same segment of an ice core, it is obviously preferable to base the identification of annual layers on all the available data [Johnsen et al. 1992; Meese et al., 1997; Alley et al., 1997; Anklin et al., 1998]. This is especially true when the available data series cannot be guaranteed to be pure annual signals, but

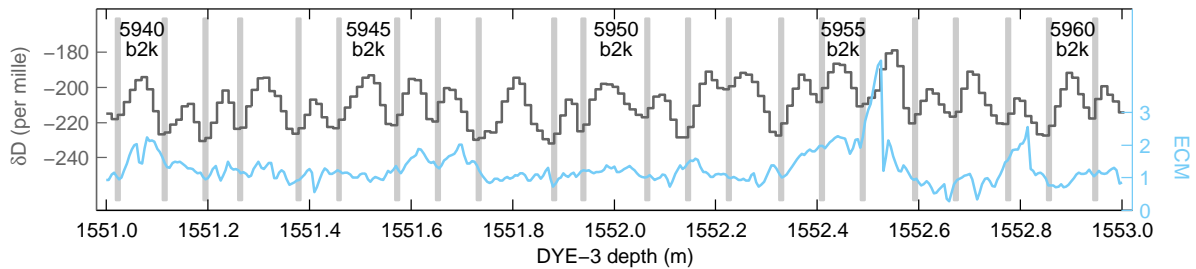


Figure 2. A section of new δD data used for the revision of the DYE-3 time scale (dark grey), together with the ECM data (blue) used in the construction of the former DYE-3 time scale of Hammer et al. [1986]. The annual layer markings of the revised time scale are shown by light grey vertical bars (dates are relative to A.D. 2000, denoted b2k).

contain contributions from other processes than those generating the annual pattern. For example, the concentration of NH_4^+ in the Greenland ice cores exhibits clear annual variations in the Holocene and in the Bølling interstadial, but the annual signal is occasionally obscured by high peaks originating from e.g. biomass burning events. The use of multiple data series thus improves the quality of the time scale produced by making the identification of annual layers more robust. However, multi-parameter data sets with a resolution sufficient for annual layer counting are sparse, and are seldom available from the brittle part of ice cores, where internal cracks in the ice make it virtually impossible to obtain uncontaminated continuous measurements of the impurities in the ice. This is one of the main reasons why multi-parameter CFA measurements have only been carried out below the depth of 1300 m in the GRIP core and below 1400 m in the NGRIP core. Because of the relatively low accumulation rate at the NGRIP drill site, $\delta^{18}\text{O}$ data from NGRIP are not optimal for identification of annual layers, while for the GRIP core, $\delta^{18}\text{O}$ measurements are not available with sufficient resolution to allow identification of annual layers in the 4–8 ka part of the core.

Due to the relatively high accumulation rate at DYE-3, stable isotope ratios from the DYE-3 ice core thus remain, in the opinion of the authors, the best ice core data available for dating the most recent 8 ka. However, at the time when the DYE-3 time scale of Hammer et al. [1986] was constructed, highly resolved stable isotope ratios had only been measured continuously down to 5.9 ka b2k, and the time scale was therefore to some degree based on interpolation and on ECM measurements below this [Hammer, 1989]. However, the highly resolved DYE-3 isotope ratio profile has recently been completed [Vinther et al., 2006]. Using the complete DYE-3 isotope data set together with GRIP $\delta^{18}\text{O}$ data in the 0–3.8 ka b2k interval and NGRIP $\delta^{18}\text{O}$ data in the 0–1.9 ka b2k interval, a new and much more robust cross-validated time scale for the DYE-3, GRIP, and NGRIP ice cores reaching just beyond the 8.2 ka cold event has been constructed [Vinther et al., 2006]. Figure 2 shows one of the new sections of DYE-3 δD data from around 6 ka b2k together with the corresponding ECM data initially used to construct the DYE-3 time scale. It is seen that the annual layers are clearly identifiable from the δD data without diffusion correction, and it is apparent that the counting error is reduced significantly compared with the uncertainty of the previous dating. The most recent 1.9 ka have been dated with no cumulated uncertainty as the reference horizon of Vesuvius (A.D. 79) is dated accurately from historical records. In the 1.9–3.8 ka b2k section the GRIP and DYE-3 records were matched using common ECM events, and the annual layers were identified from the combined records. The maximum counting error is therefore very small, estimated to about 0.25%. In the 3.8–8.3 ka b2k section the time scale is based on DYE-3 stable isotope ratios, as illustrated in Figure 2. In

the 3.8–6.9 ka b2k part, the estimated maximum counting error is 0.5%. At the DYE-3 drill site, diffusion of the oxygen isotopes in the ice affects the annual signal when the annual layer thickness is below 6 cm. Due to ice-flow induced thinning, the mean annual layer thickness is reduced to about 6 cm at a depth of 1625 m (corresponding to 6.9 ka b2k). From 6.9 to 8.3 ka b2k the maximum counting error therefore increases to 2%, because the annual signal gradually is weakened by diffusion in the ice. In this way, the new time scale reaches beyond the 8.2 ka cold event with a cumulated maximum counting error of about 50 years. The maximum counting error has been estimated from the number of potential annual layers that were hard to interpret, and does not include a possible bias in the annual layer identification process. The concept of maximum counting error will be discussed further in section 5.1.4.

A prominent ECM double peak is found close to the deepest part of the $\delta^{18}\text{O}$ -minimum of the 8.2 ka cold event [Hammer et al., 1986]. The layer is characterized by a high fluoride content, and can thus most likely be attributed to an Icelandic volcano. Because of the special timing of the ECM double peak inside the $\delta^{18}\text{O}$ minimum, this stratigraphic horizon can be uniquely identified in all Central Greenland ice cores, and has thus been chosen as the datum of the presented time scale. According to the revised DYE-3 time scale [Vinther et al., 2006], the annual layer inside the ECM double peak has been dated to 8236 b2k with a maximum counting error of 47 years. Any future changes in the dating of this horizon will propagate to the presented GICC05 time scale. The depths of this horizon in the Central Greenland deep ice cores are listed in Table 2.

4.1. Multi-parameter Annual Layer Counting in the GRIP Ice Core (Holocene I section)

Below 8.3 ka b2k, the resolution of the DYE-3 isotope signal becomes insufficient for annual layer identification due

Table 2. Depth of the ECM double peak inside the 8.2 ka event in selected Greenland ice cores^a

Ice core	Depth (m)
NGRIP1	1228.67
NGRIP2	1228.24 ^b
GRIP	1334.04
DYE-3	1691.06
GISP2	1392.66

^a The peak serves as the datum of the presented time scale and is assigned the age 8236 b2k with a maximum counting error of 47 years [Vinther et al., 2006].

^b Estimated using the calculated offset of 0.43 m between NGRIP1 and NGRIP2 as described in section 2.

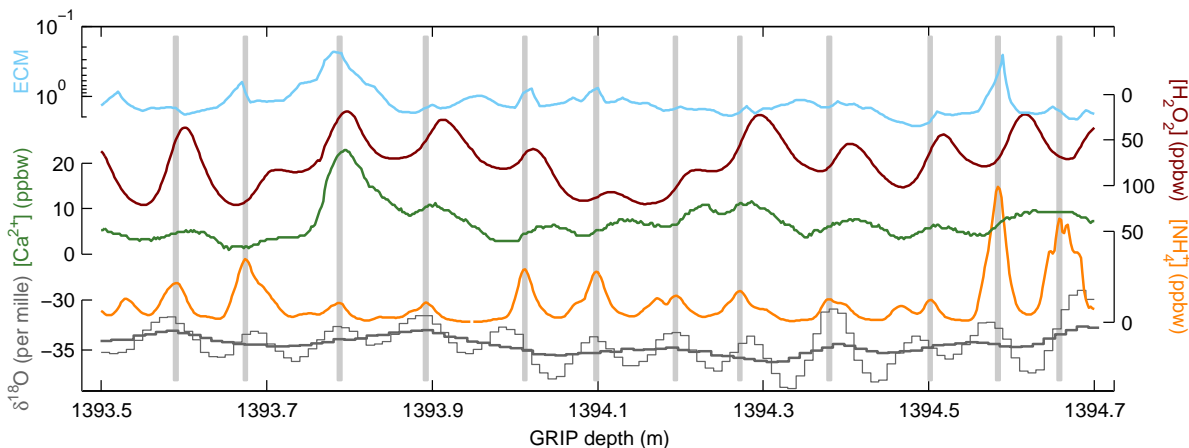


Figure 3. Example of 1.2 meter of GRIP data and annual layer markings (grey vertical bars) from about 8.8 ka b2k. The annual layers are identified as matching pairs of spring and summer indicators: spring is characterized by high dust content leading to peaks in $[\text{Ca}^{2+}]$ and dips in the $[\text{H}_2\text{O}_2]$ curve, while summer is characterized by high $[\text{NH}_4^+]$ and corresponding minima in the ECM curve. Note that the ECM and $[\text{H}_2\text{O}_2]$ curves are plotted on reversed scales. In this section the annual layer identification procedure is supported by high-resolution $\delta^{18}\text{O}$ data, corrected for diffusion using the method of Johnsen [1977] and Johnsen et al. [2000] (raw data: thick line, diffusion corrected data: thin line).

to flow-induced thinning of the layers, and the GRIP isotope signal is so severely dampened by diffusion that identification of annual layers from the isotope profile alone is dubious. Instead, annual layers were identified from the CFA data set of Fuhrer et al. [1993; 1996; 1999], which has already provided the GRIP core with a stratigraphic time scale covering the period from 7.9 ka b2k to the YDPB transition [Johnsen et al., 1992]. An initial comparison of this time scale with the new NGRIP data (see below) indicate that the existing GRIP time scale is missing a significant number of annual layers in the Holocene II section, and a new GRIP chronology has therefore been constructed using the $[\text{NH}_4^+]$, $[\text{H}_2\text{O}_2]$, and $[\text{Ca}^{2+}]$ series obtained by Fuhrer et al. [1993; 1996; 1999], ECM data, and short sections of high-resolution isotope data (5 meter of data for every 50 meters).

In general the $[\text{Ca}^{2+}]$ series has fewer peaks than the $[\text{NH}_4^+]$ series, which at least partially arises from the fact that the $[\text{Ca}^{2+}]$ measurements have a significantly lower resolution (see table 1). When originally marking the annual layers in the GRIP core, the $[\text{Ca}^{2+}]$ series was believed to be the most reliable for annual layer identification, while the $[\text{NH}_4^+]$ series was considered to contain additional peaks not related to the annual signal. If on the other hand all significant peaks in the $[\text{NH}_4^+]$ signal are counted as years, the number of annual layers increase by about 7%. The approach used here is based on the different seasonality of the series as described in section 3: the spring is characterized by high dust content leading to high $[\text{Ca}^{2+}]$ and dips in the $[\text{H}_2\text{O}_2]$ curve, while the $[\text{NH}_4^+]$ has summer maxima and corresponding ECM minima. The annual layers have been defined as matching pairs of these spring and summer indicators, which is supported by the high resolution $\delta^{18}\text{O}$ data where available. One of these sections is shown in Figure 3. The fact that the dust-rich spring is observed in both the $[\text{Ca}^{2+}]$ and $[\text{H}_2\text{O}_2]$ curves, while the summers are seen in both the $[\text{NH}_4^+]$ and ECM curves reduces the counting error significantly as measurement-related problems and resulting data gaps often affect only one series at a time. When either the spring or summer indication is weak, or when the relative timing of the spring and summer indicators is unusual, an "uncertain layer mark" has been placed. From the start it was agreed between the investigators that the uncertain marks should

be regarded and counted as "half years", and the uncertain marks have therefore been set with this in mind. The validity of the applied criteria has been tested by marking annual layers in the Holocene II section using GRIP data only, and subsequently cross-validating with the NGRIP annual layer sequence. Differences smaller than 1% were observed, and the criteria used in the GRIP and NGRIP parts are therefore considered to be consistent.

In practice, the time scale was constructed by first letting three investigators (BMV, JPS, and SOR) independently place annual layer marks. The three annual layer profiles were different in around 200 places in the 2.4 ky long section, but the total number of annual layer marks in the three profiles agreed within 1.5%. Each point of disagreement was subsequently reviewed with a fourth investigator (HBC) acting as arbitrator. The resulting time scale represents a compromise between the three initial versions, using uncertain layer marks to mark points where unanimity could not be reached, or where either the spring or summer indicators are not clear. The resulting time scale contains about 1.5% more annual layers than the previous counted GRIP scale in the Holocene I section [Johnsen et al., 2001].

4.2. Multi-parameter Annual Layer Counting in the NGRIP Ice Core

The NGRIP data set comprises an extensive set of measurements, where a clear annual signal is present in up to 9 parallel data series. As an initial approach, three investigators (KKA, AMS, and JPS) made independent annual layer counts based on all available NGRIP data series. In the Holocene, Allerød, and Bølling periods, the investigators agreed within a few percent on the number of annual layer marks, and in many century-long sections they agreed on every year, but in the Younger and Oldest Dryas discrepancies of up to 5% and 10%, respectively, were observed. The differences were most pronounced in the coldest periods where thin annual layers begin to appear as shoulders on neighbouring peaks, and around sharp transitions. Again the three initial time scales were reviewed with a fourth investigator (SOR) acting as arbitrator, thereby producing a time scale where every annual layer marking was acceptable by all investigators. Ambiguous features and points, where unanimity could not be reached, were marked by uncertain layer marks.

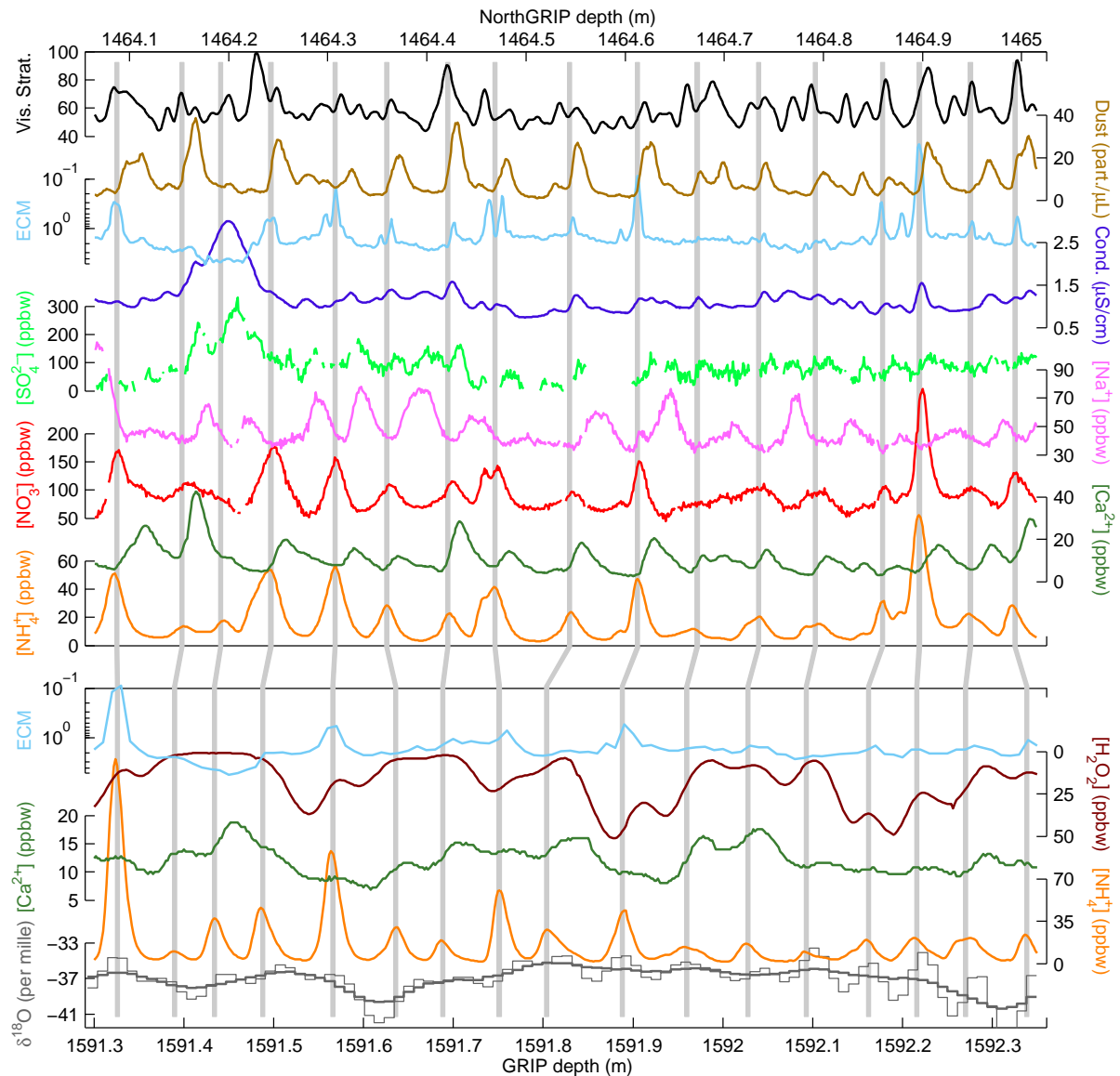


Figure 4. Example of data and annual layer markings (grey vertical bars) from the early Holocene. The upper nine panels show a 0.95 meter long section of NGRIP data, and the lower five panels show the corresponding 1.05 m section in the GRIP data set. The annual layers are marked at the summer peaks, which are defined by high $[\text{NH}_4^+]$ and $[\text{NO}_3^-]$. The spring is characterized by high dust mass leading to peaking $[\text{Ca}^{2+}]$ and dips in the $[\text{H}_2\text{O}_2]$ profile, while the $[\text{Na}^+]$ peaks in late winter. The visual stratigraphy profile does not contain clear annual layers, but contains peaks corresponding to almost every dust peak. The ECM (note the reverse logarithmic scale) anti-correlates strongly with the largest peaks in $[\text{NH}_4^+]$, but does not itself allow safe identification of annual layers. The lower four panels show the same time interval in the GRIP core, from which $[\text{Ca}^{2+}]$ and $[\text{NH}_4^+]$ measurements exist [Fuhrer et al., 1993; 1996; 1999]. The similarity of the $[\text{NH}_4^+]$ records (and consequently also to some degree the ECM records) from NGRIP and GRIP allows a close stratigraphic matching of the two cores. The annual layer identification has been based on impurity data only, but is supported by comparison with high-resolution $\delta^{18}\text{O}$ data that are available for a few short sections in the Holocene. The $\delta^{18}\text{O}$ data have been corrected for diffusion using the method of Johnsen [1977] and Johnsen et al. [2000] (raw data: thick line, diffusion corrected data: thin line)

4.2.1. Holocene II Section, NGRIP Depth 1404.7–1492.45 m

In the Holocene, the series show strong and different seasonality as described in section 3 and illustrated in the upper part of Figure 4. Slightly different relative timing of the different species is often observed for one or two years, most often related to apparent merging of successive seasons, where e.g. winter and spring peaks or spring and summer

peaks occur simultaneously as observed in Figure 4, where the $[\text{Na}^+]$ winter peak and the following $[\text{Ca}^{2+}]$ and dust spring peaks occur at the same depth of 1464.87 m. The fact that the different series have different seasonality makes it highly improbable that full years are missing in the data set due to post-depositional processes or missing precipitation, and also makes the identification of annual layers very robust. Of the 1436 annual layers marked in this section,

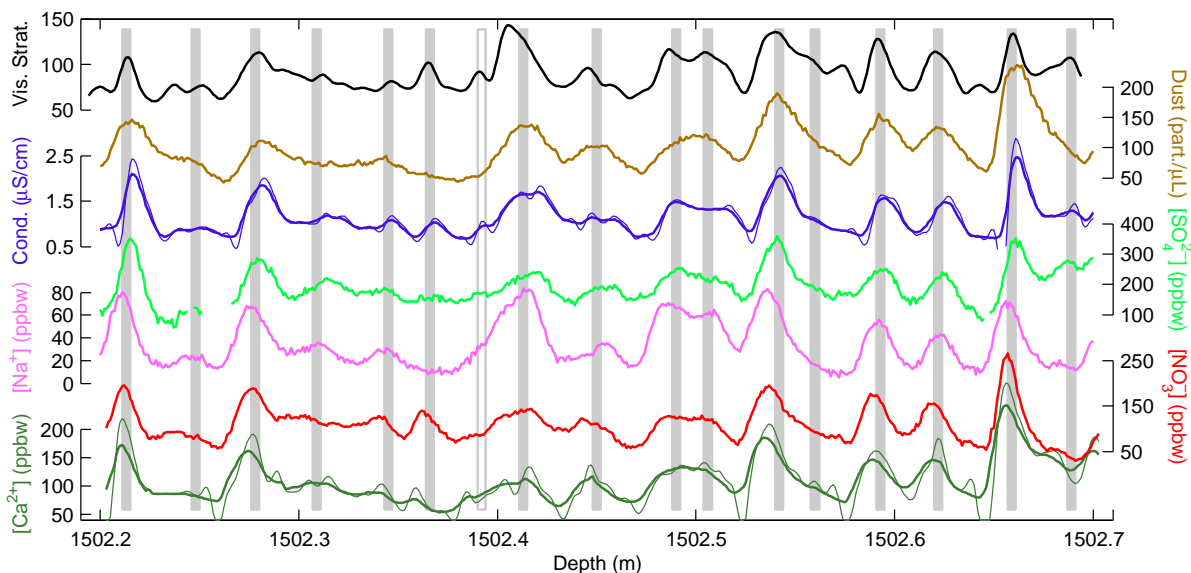


Figure 5. Example of data (heavy lines), resolution enhanced data (thin lines), and annual layer markings (grey bars) from the Younger Dryas. The different series peak almost simultaneously, and peaks in the VS profile are seen to be connected closely to the annual layers. However, too many layers could easily be counted if the counting was based on VS data alone, emphasizing the importance of using multiple data series for annual layer counting. The uncertain layer (open grey bar) at 1502.39 m is a potential thin annual layer, not fully resolved by the measurements.

only 23 marks, or 1.6%, were marked as uncertain layers. Of these 23 marks, 20 are placed where some series indicate that an annual layer is present, while other series do not have evidence of a layer. The remaining 3 uncertain layers are caused by data gaps or short sections with data quality problems.

GRIP CFA data are also available in the Holocene II section, and the GRIP and NGRIP cores can be matched on an annual basis by first using major ECM horizons to provide a low-resolution stratigraphic matching of the two records and then by matching the $[\text{NH}_4^+]$ profiles of the two cores year by year in between the fix points. In Figure 4, the NGRIP data (upper nine panels) are presented together with the corresponding $\delta^{18}\text{O}$, $[\text{NH}_4^+]$, $[\text{Ca}^{2+}]$, $[\text{H}_2\text{O}_2]$, and ECM series from GRIP (lower five panels). In order to be able to assess the possible bias of the annual layer counting procedure, two investigators (BMV and HBC) constructed a time scale for the Holocene II period using the combined data set of CFA and ECM data from both NGRIP and GRIP independently from the four-investigator NGRIP time scale described above. The question of possible bias will be discussed further in section 5.1.4.

4.2.2. Younger Dryas Section, Depth 1492.45–1526.52 m

During cold periods like the Younger Dryas, those series showing annual cycles mostly peak simultaneously. This supports the conclusions of Werner et al. [2000] that point to that Central Greenland receives only little winter precipitation under glacial conditions. Although there is roughly one $[\text{NH}_4^+]$ peak per year on average, the $[\text{NH}_4^+]$ signal was not in general regarded as being reliable for annual layer identification in the Younger Dryas. Also the ECM signal becomes very hard to interpret in some sections. In the Younger Dryas, the expected mean annual layer thickness derived from flow modeling is less than twice the wavelength of the shortest cycle that can be resolved by the CFA measurements. Thus, thin annual layers may be poorly resolved or in exceptional cases vanish. When identifying the annual layers, special consideration was put into identifying features that could represent two almost merged layers. In Figure 5 the usable data series (original and resolution enhanced) are shown together with the annual layer markings.

The uncertain layer at depth 1502.39 m could possibly be a thin annual layer that cannot be fully resolved, but may also just arise from unusually shaped annual peaks.

1232 annual layers are marked in the Younger Dryas, of which 78 are uncertain. The uncertain layers fall in two categories: layers that are only supported by evidence in some of the series (type I), and as the one illustrated, shoulders, wide peaks, or double peaks that could represent two thin annual layers not fully resolved or one annual layer represented by peaks with unusual shapes (type II). Type II layers account for almost 3/4 of the uncertain layers in the Younger Dryas.

4.2.3. Bølling and Allerød Sections, Depth 1526.52–1604.64 m

The Bølling and Allerød sections proved to be the most challenging section to date, due to the very changeable nature of the data (and climate) in this time interval. Stable isotope data show that climatic conditions generally change from a rather warm climate at the beginning of the Bølling to a much cooler climate at the end of the Allerød, but also that the temperature changes abruptly towards both cooler and warmer conditions several times during this period. This variability is clearly observed in all data series. The seasonality of the series changes rapidly several times; from conditions similar to those in the Younger Dryas, where all series peak simultaneously, to Holocene-like conditions where the series have different seasonality. These changes do not always happen synchronously with changes in the concentration levels, isotopic values, or observed annual layer thickness. A detailed study of the different timing of the changes in the different data series can increase the understanding of the physical processes governing the climate system, but this is beyond the scope of this work. However, the observed changes of the properties of the data make the identification of annual layers difficult, even when all data series are available.

In the warmer parts of Bølling and Allerød, the $[\text{NH}_4^+]$ series proves useful for dating, as observed in the Holocene. The VS and conductivity series show clear annual cycles in the sections where most series peak simultaneously. The $[\text{NH}_4^+]$

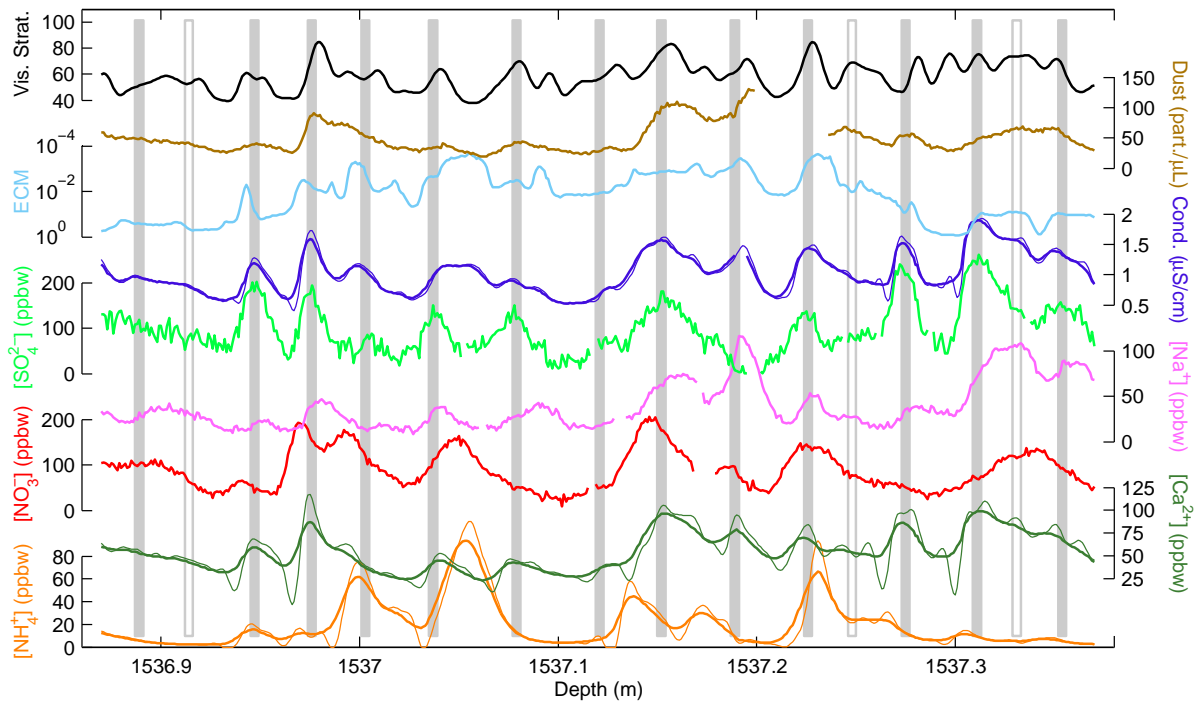


Figure 6. Example of data (heavy lines), resolution enhanced data (thin lines), and annual layer markings (grey bars) from a cold period in Allerød. In this section the $[\text{NH}_4^+]$ and $[\text{NO}_3^-]$ series do not show clear annual cycles, while the other series peak almost simultaneously. The open grey bars indicate uncertain layers. The annual layer marks have been set in the annual peaks of $[\text{Ca}^{2+}]$.

and $[\text{NO}_3^-]$ series are observed to have a peculiar tendency to contain additional simultaneous summer peaks not present in the other series, a phenomenon not encountered elsewhere in the data used in this work. In Figure 6, a section from a relatively cold part of Allerød is shown. It is apparent that the relative timing of the different series is less constant

than in the Holocene and Younger Dryas. Note also how the $[\text{NH}_4^+]$ and $[\text{NO}_3^-]$ series have roughly the same number of peaks as the other series, but without exhibiting a clear annual cycle, and that the dust mass series only barely resolves the annual cycle. The ECM does not show clear annual cycles, and there are substantially more peaks in VS

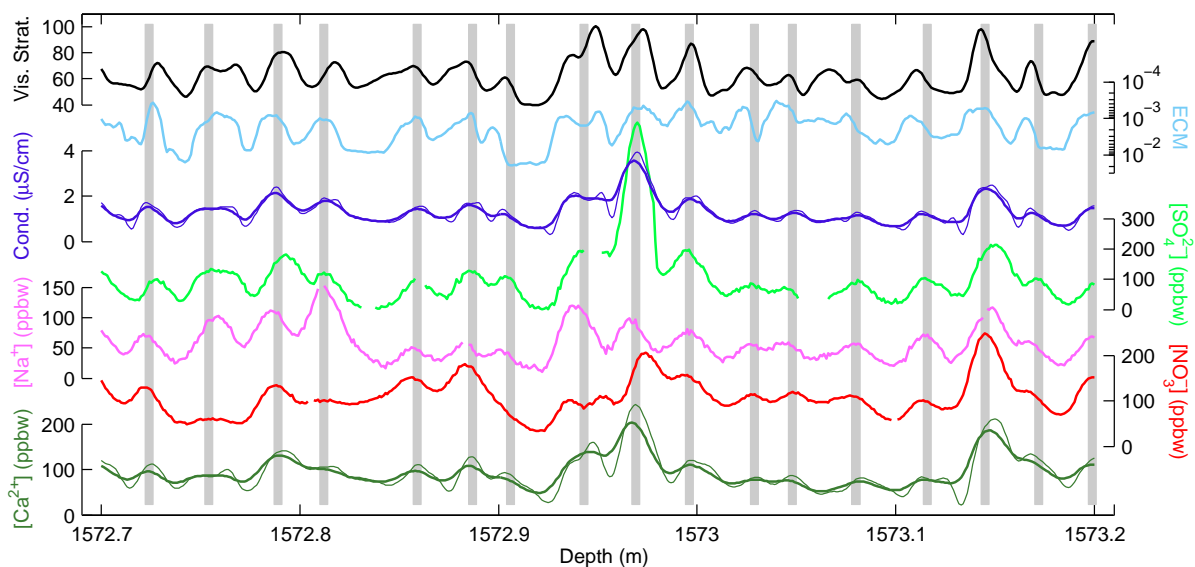


Figure 7. Example of data (heavy lines), resolution enhanced data (thin lines), and annual layer markings from the cold period between Bølling and Allerød (MIS-1d), with $\delta^{18}\text{O}$ values close to that of the section shown in Figure 6. However in this section, all series peak simultaneously, and there are no variations in seasonality. The $[\text{NO}_3^-]$ and ECM series show clear annual cycles, and the annual layers could be identified with reasonable certainty based on the ECM and VS series alone. The $[\text{NH}_4^+]$ signal is not shown, as it does not exhibit a clear annual signal.

than those associated with the annual layers. A section at the boundary between Bølling and Allerød (inside MIS-1d) is shown on Figure 7. It is also a relatively cold period, having $\delta^{18}\text{O}$ -values only slightly higher than those in the Allerød section in Figure 6. The dust and $[\text{NH}_4^+]$ series have been excluded, as they do not show annual cycles, while the $[\text{NO}_3^-]$ and ECM series again are showing clear annual cycles. Note also how the series peak almost simultaneously, and that the annual layers can be placed based almost on the ECM and VS series alone. The sections in Figures 6 and 7 would be expected to be rather similar from their isotopic values alone, but the differences clearly illustrate the challenges of identifying annual layers in periods with highly variable climatic conditions.

Of the 1843 annual layer markings in the Bølling and Allerød, 94 are uncertain layers. About 10 are placed to mark layers that are uncertain because of data quality problems and data gaps, and the rest are equally divided between the two types defined in section 4.

4.2.4. Oldest Dryas Section, Depth 1604.64 m and below

In the Oldest Dryas, the phasing of the series is similar to the phasing observed in the Younger Dryas. When comparing the data resolution with estimated model annual layer thicknesses from the ss09sea model of NGRIP members [2004], it is apparent that the resolution is marginal in the Oldest Dryas. An inspection shows that the data series do indeed contain many double peaks, wide peaks, and shoulders suspected to contain additional annual layers. As the initial approach, we use the same criteria as in the Younger Dryas, marking the most prominent of these features with two annual layer markings and the less pronounced with an annual layer marking plus a type II uncertain layer marking. However, it is clear that many weak indications remain in the data that could possibly represent additional annual layers. Because of the marginal resolution of the CFA data, more emphasis has to be put on the highly resolved VS and ECM data series, and only the last few meters of the Oldest Dryas before the transition into Bølling have therefore been included in the presented time scale. The time scale for these few meters is slightly less reliable, but because of the shortness of the section (87 marks, of which 7 are uncertain), and the fact that the isotope values (and thus the expected annual layer thickness) do not attain full glacial values, the problem is of minor importance.

5. Constructing the Final Time Scale

As described in section 4, the datum of the presented time scale is the volcanic horizon inside the 8.2 ka cold event dated in the DYE-3 ice core to 8236 b2k with a maximum counting error of 47 years. In the Holocene I section, the revised time scale based on GRIP CFA data is used. The GRIP time scale has been transferred to NGRIP by matching the ECM signals of GRIP and NGRIP. The GRIP $[\text{NH}_4^+]$ series contains clear annual peaks, and because peaks in the $[\text{NH}_4^+]$ series lead to minima in the ECM signal, it is possible to match the two series on an annual scale. The matching can be ambiguous, but for every few tens of years better fix points are supplied by strong ECM peaks, primarily related to volcanism, or by recognizable patterns in the $[\text{NH}_4^+]$ and ECM curves. The mismatch is estimated to be maximum one year at fix points and maximum 3 years in long sections without fix points. The result is a common Holocene I time scale for GRIP and NGRIP starting with the year 7903 b2k (GRIP depth 1299.82 m, NGRIP depth 1194.05 m), leading up to the year 10,276 b2k (GRIP depth 1522.79 m, NGRIP depth 1404.71 m) after which the NGRIP CFA data start. In the Holocene II section, the four-investigator time scale

based on NGRIP data and the two-investigator time scale based on both GRIP and NGRIP data have been combined. The latter is constructed without uncertain layer markings, while the first one contains 23 uncertain marks. On top of the uncertain layers only present in the 4-investigator time scale, the number of years found in one but not the other time scale amounts to 9 and 7 annual layer markings, respectively. In order to reach a common result, the two time scales were compared and combined by one investigator from each group. It was agreed how to interpret the combined GRIP and NGRIP data in each of the 39 points of disagreement. The use of uncertain layer markings has been adopted for this combined time scale, and the uncertain layers were counted as 0.5 year in the construction of the final time scale. The resulting Holocene II time scale is valid for both cores, covering the age interval 10,277–11,703 b2k, and contains 6.6% more annual layers than the existing GRIP time scale [Johnsen et al., 1992]. Finally, the time scale of the Holocene I and II periods was transferred to DYE-3 depths using the same ECM-based matching procedure, making the GICC05 time scale valid for all three cores.

The annual layer counting in NGRIP continues back to a depth of 1607 m, reaching a few meters below the Oldest Dryas – Bølling transition, which is found at a depth of 1604.64 m, corresponding to an age of 14,692 b2k. As above, the uncertain marks have been counted as 0.5 year.

Below the YDPB transition, matching of the GRIP and NGRIP series becomes more difficult as the GRIP CFA fails to resolve the annuals in the Younger Dryas, and the annual cycles in the ECM signal become hard to identify. The time scale obtained from the NGRIP CFA data can therefore not readily be transferred on a year-by-year basis to the GRIP core below the YDPB transition. Work by Seierstad et al. [2006] focuses on the possibility of matching the GRIP and NGRIP records at greater depths, and on identifying annual layers based on high-resolution δD data within the Bølling-Allerød period in the GRIP core, and future progress in this work will hopefully extend the time range where GRIP data is available on the GICC05 time scale.

5.1. Assessing the Uncertainty

Contributions to the uncertainty of a stratigraphic ice core time scale include problems with the core stratigraphy, core loss during drilling and handling, data loss during sampling and measurements, insufficient measuring resolution, and misinterpretation of the annual layer record [Alley et al., 1997].

5.1.1. Uncertainty from Imperfect Core Stratigraphy

The basic assumption that the ice core comprises an unbroken sequence of precipitation from the past can be erroneous due to missing precipitation or due to post-depositional processes like re-deposition or melting. The relatively high accumulation rates and small surface slopes make loss of full years due to missing precipitation or wind scouring unlikely [Fisher et al., 1983], and melt events are known to occur only extremely rarely at the GRIP and NGRIP drill sites. In the 1400 year long Holocene II section where both GRIP and NGRIP CFA data exist, the records were matched year to year, and no indication of missing years was found when comparing the records, substantiating the assumption of the ice cores being unbroken annual layer sequences. This is also supported by the discussion in section 6. In cold periods with lower accumulation, and possibly more stormy conditions, this may not be true, but the uncertainty contribution from imperfect core stratigraphy is considered to be insignificant in the time periods spanned by this work.

5.1.2. Uncertainty from Data Gaps

In the depth interval considered in this work, core loss is nonexistent, and only very short sections of the NGRIP core could not be sampled for the CFA measurements. Around

irregular core breaks, the ends of the CFA sample pieces had to be trimmed, resulting in a few centimeters of missing CFA data, but VS and ECM measurements are often available across these short CFA data gaps. Most of the gaps are less than a centimeter long, not causing ambiguities in the process of annual layer identification. Longer data gaps of 2–10 cm (corresponding to about once or twice the mean annual layer thickness) occur on average every five meters or so, but using the ECM and VS data, it is usually possible to place the annual layer markings without significant uncertainty. In addition to the short sections where all CFA data are missing, one or more of the CFA series are sometimes missing over longer intervals due to problems with one or more of the analysis subsystems. In the cases where annual layer identification has been difficult due to missing data series, the uncertainty has been indicated by using uncertain layer marks. The total uncertainty due to missing data is thus estimated to be around ten years out of the 4000–5000 years spanned by the NGRIP data in this work, and most of the uncertainty is accounted for by the use of uncertain layer markings.

In the GRIP Holocene I section there are occasional CFA data gaps affecting one or two of the series, totalling about 10 m, plus a number of smaller gaps which do not cause problems for the annual layer identification. Most of the longer gaps contain 2–4 annual layer marks, but the uncertainty contribution is small because all species are not missing at the same time, and because ECM data are available across the CFA data gaps. The estimated total uncertainty contribution from data gaps is a few per mille, of which the major part is accounted for via the use of uncertain layer marks.

5.1.3. Uncertainty from Insufficient Measuring Resolution

The combined CFA, ECM, isotope, and VS data set is believed to resolve the annual layers well in the Holocene and in the warm parts of the Bølling and Allerød, while extraordinarily thin annual layers may show up only faintly or be lost in the Younger Dryas and in the coldest parts of the Allerød period.

In the Holocene section, only a couple of features that could represent poorly resolved layers were identified. These were marked with uncertain layer marks. It is not considered to be likely that a significant number of years have vanished completely due to insufficient resolution.

Double peaks suspected to contain more than one year are much more common in the Younger Dryas section. In addition, a small number of years may have been lost altogether due to insufficient resolution at the end of Allerød and in the Younger Dryas. Special care was taken not to miss thin layers represented as poorly separated double peaks or shoulders on neighbouring peaks. Depending on the amount of evidence present, these features were marked as two layers or as a layer and an uncertain layer. The upper limit of the number of lost layers is estimated to be a few tens of years in the section comprising the Younger Dryas and the end of Allerød, corresponding to about 1% of the section's annual layers.

5.1.4. Uncertainty from Erroneous Interpretation of the Annual Layer Record

The vast majority of annual layers stand out clearly in all data series, but uncertainty is introduced when an annual layer is backed up by evidence only in some of the data series, or when a certain well-resolved feature is suspected to contain more than one annual layer. Also, the basic assumption that the annual layers in ice cores are represented by peaks in almost all the individual data series may not be perfectly true. This uncertainty contribution is the dominant part of the total uncertainty, but can only be partially assessed

quantitatively. The cases of ambiguity in the annual layer identification process have been identified using the uncertain layer markings, but in addition one must expect that there can be a bias in the annual layer identification process. This is clearly illustrated by the result of the revision of the GRIP Holocene time scale. As described in section 4.1 and 5, the number of annual layers in the Holocene I and II sections have increased by 1.5% and 6.6% from the old to the new GRIP time scale, respectively. These differences reflect a change in the way data are interpreted, rather than counting errors, which is reflected by the fact that the increase in the number of annual marks in the Holocene II section is 4–5 times larger than the number of uncertain layer marks in the same section.

The comparison of the 2-investigator and the 4-investigator time scales of the Holocene II section constitutes the only place where we can make an independent bias magnitude estimate. The two time scales were made using partially the same data, but the two groups of investigators worked independently of each other. The differences are described in section 5, and indicate a bias level of 1% or less in the Holocene II section. Below the YDPB transition, we do not have the opportunity of checking the time scale with independent ice core data, and thus only aim at estimating the maximum counting error, which we derive from the number of uncertain layer marks. Over the total depth interval in question here, 294 of 7021 annual layer marks (corresponding to 4.2%) were of the uncertain type. As the uncertain layer marks are regarded as 0.5 ± 0.5 year in the final time scale, the number of years in the section is 6874 with a maximum counting error of 147 years assuming that the counting errors are correlated. In Table 3, the number of layer markings within each climatic period are listed together with the maximum counting error derived from the number of uncertain layer markings in this way. The counting error derived from the uncertain layer markings heavily depends on whether the uncertainties are assumed to be correlated or uncorrelated, and

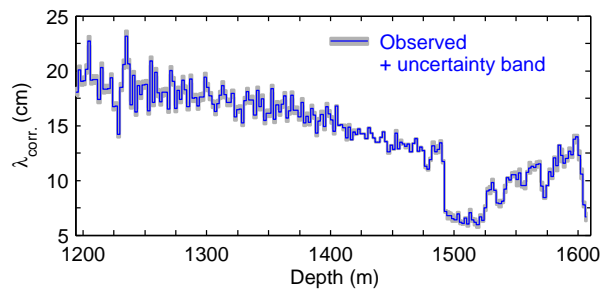


Figure 8. Observed annual accumulation rates after strain correction, λ_{corr} , averaged over 2 meter sections. The shaded uncertainty band is derived from the uncertain annual layer marks (in the Holocene II and glacial parts), and thus represents only the part of the uncertainty that is related to ambiguous features in the data set. In the Holocene I section, a constant 2% uncertainty band is used. The high variability of λ_{corr} in the Holocene I section is likely to be caused by a combination of two effects: (1) at smaller depths each 2 meter interval contains fewer annual layers resulting in increased scatter around the mean value, and (2) the transfer of the GRIP data based time scale to NGRIP depths using common ECM fix points introduces an uncertainty in the number of annual layers in each 2 meter interval, and thus in the derived accumulation rates, although the total number of annual layers remains accurate. The accumulation rates are sensitive to how the strain correction is performed, and should be regarded as preliminary results.

Table 3. Estimated maximum counting error excluding possible bias in the annual layer identification process for the different climatic periods.

Section	NGRIP depth (m)	Number of annual layers Certain	Uncertain	Duration (y)	Maximum counting error absolute (y)	relative
Holocene I	1194.05–1404.74 ^a	2326	96	2374	48	2.0%
Holocene II	1404.74–1492.45	1418	19	1427	10	0.67%
Younger Dryas	1492.45–1526.52	1154	78	1193	39	3.3%
Allerød	1526.52–1574.80	1147	61	1178	31	2.6%
Bølling	1574.80–1604.64	602	33	618	17	2.7%
End of Oldest Dryas	1604.64–1607.00	80	7	84	4	~ 4%
Total		6727	294	6874	147	2.1%

^a Time scale based on GRIP CFA data, corresponding GRIP depths: 1299.81–1522.75 m.

consequently on which error summation procedure should be applied. If the counting errors are assumed to be fully uncorrelated, the errors should be summed in a quadratic sense, producing a maximum counting error estimate of $\sqrt{\left(\frac{1}{2}\right)^2 + \dots + \left(\frac{1}{2}\right)^2} = \sqrt{294 \left(\frac{1}{2}\right)^2} = \frac{\sqrt{294}}{2} \approx 9$. Using the more reasonable assumption that the errors are fully correlated within each climatic period and uncorrelated from one period to the other, the maximum error estimate becomes $\sqrt{48^2 + 10^2 + 39^2 + 31^2 + 17^2 + 4^2} = 72$, using the period division from Figure 1. This approach was also used when deriving counting error estimates for the previous GRIP time scale, but has the obvious disadvantage that the maximum counting error estimate depends on the choice of which periods are considered independent. If for example the Allerød period is considered to consist of 4 independent periods (corresponding to the GIS1a–e of Björck et al. [1998]), the 61 uncertain layer marks only result in a maximum

counting estimate of $\sqrt{\left(\frac{9}{2}\right)^2 + \left(\frac{10}{2}\right)^2 + \left(\frac{38}{2}\right)^2 + \left(\frac{4}{2}\right)^2} \approx 20$ years instead of 31 years if Allerød is considered to be one period. Recognizing that the counting errors in reality are neither uncorrelated nor fully correlated, we adopt the simple and conservative approach, summing up the uncertainties as if they were correlated. The counting error estimates presented here are thus highly conservative, and as the maximum counting error dominates over the sources of uncertainty associated with imperfect stratigraphy and data gaps by about an order of magnitude, only the maximum counting error is given. The uncertainty from bias in the annual layer identification process can by the nature of the problem not be estimated without the existence of independent data sources, and is thus not included in the error estimates presented.

6. Distribution of Annual Layer Thicknesses

Figure 8 shows the annual layer thickness profile derived from the NGRIP core using the GICC05 time scale. The uncertainty band indicated in the figure is derived from the uncertain layer marks, and thus represents the part of the uncertainty that arise from features in the data that the investigators found ambiguous. The strain correction has been performed using a first order flow model, where the strain ϵ at depth z is given as $\epsilon = 1 - \frac{z}{z_0}$. The value $z_0 = 2680$ m is used, whereby ϵ closely resembles the strain history derived from the ss09sea model [NGRIP members, 2004] in the 1200–1600 m depth interval. As the ss09sea model time scale is significantly different from the GICC05 time scale in this interval, the absolute accumulation rate values should therefore be regarded as preliminary. However, the ratios between the accumulation rates in the Holocene II, Younger Dryas, and Bølling periods are robust to a wide range of reasonable z_0 values.

Distributions of strain corrected observed annual layer thicknesses within three selected periods are shown in Figure 9 (note the logarithmic scale). To ensure that the climatic conditions are rather constant within each period, the variable Allerød period has been excluded, and a few meters at each end of the periods have been removed to ensure that the transitions between the individual periods do not influence the distributions. It is apparent from the figure that the annual layer thicknesses to a good approximation are log-normally distributed, and that the variability of the annual layer thicknesses is by far smallest in the Holocene II section, and roughly identical for the Younger Dryas and Bølling sections. If the conclusion that annual layer thicknesses are log-normally distributed holds in general, mean and standard deviation values of accumulation rates should be calculated from logarithmic transformed data rather than from the observed annual layer thicknesses, contrary to common usage, because the notion of standard deviation makes more sense when calculated for data that are approximately symmetrically distributed. Using the mean accumulation rate

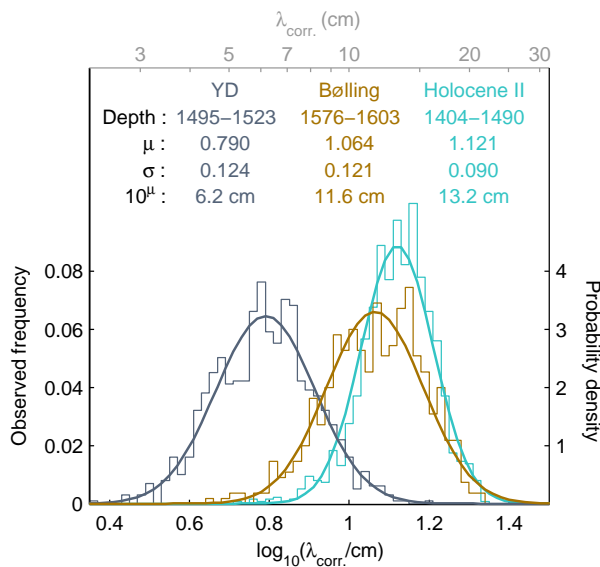


Figure 9. Distribution of strain corrected annual layer thicknesses λ_{corr} in the Holocene II, Younger Dryas and Bølling periods (thin lines). The distributions of $\log(\lambda_{corr})$ in each of the three periods are close to Gaussian distributions (thick lines). The coefficients of the fitted Gaussian curves are listed. The annual layer thickness is thus seen to have a log-normal distribution, and the chances of encountering an annual layer with half and double the mean thickness, respectively, are thus equal (see section 6). The mean accumulation rates (the 10^μ values) derived from the fitted curves are sensitive to how the strain correction is performed, and should be regarded as preliminary results.

Table 4. Age and maximum counting error estimates for selected horizons^a

Horizon	NGRIP depth (m)	Age (b2k)	Total maximum counting error (y)
Upper limit of presented time scale	1194.05	7,903	41
Time scale datum (8.2 ka cold event)	1228.24	8,236	47
Saksunarvatn volcanic layer	1409.83	10,347	89
YD – Preboreal transition	1492.45	11,703	99
Vedde volcanic layer (Z1)	1506.14	12,171	114
Onset of Younger Dryas	1526.52	12,896	138
End of Bølling	1574.80	14,075	169
Onset Bølling	1604.64	14,692	186
Lower limit of presented time scale	1606.96	14,776	190

^a The total maximum counting error consists of a maximum counting error derived as described in section 5.1.4 plus the 41 year maximum counting error from the dating of the upper 7.9 ka in the DYE-3 ice core, but does not include possible bias in the annual layer identification process. All ages are reported relative to A.D. 2000 (b2k).

values derived from the fitted log-normal curves of Figure 9, the accumulation rate in the Younger Dryas and Bølling periods are 47% and 88% of the Holocene II value, respectively, or 48% and 89% of the Holocene II values if ordinary mean values are used. These ratios are robust within $\pm 1\%$ for $z_0 \in [2580, 2780]$ m. Although the strain profile derived from the ss09sea model is not fully consistent with the GICC05 time scale, the inaccuracy of the strain profile is regarded to be smaller than the effect of varying z_0 within the bounds described, and we thus regard the accumulation rate ratios presented to be precise at least within $\pm 2\%$. The ratios indicate a smaller contrast between the stadial and interstadial accumulation rates than those observed in the GISP2 ice core where the similar ratios are approximately 43% and 97% [Alley et al., 1993; Cuffey and Clow, 1997]. Being log-normally distributed, annual layers with e.g. double and half the mean annual thickness λ_{mean} , respectively, will occur with equal probabilities. Using the fitted distributions, the probability of a random annual layer being either thicker than $2\lambda_{mean}$ or thinner than $\lambda_{mean}/2$ can be estimated to be below 0.1% for the Holocene II section, 1.5% for the Younger Dryas, and 1.3% for Bølling. When compared with the resolution of the data used in this work, the distribution of the annual layer thicknesses for the Holocene II section indicates that it is extremely unlikely that any annual layers have been missed in the Holocene parts of this work due to insufficient resolution, and that the problem also should be negligible in the Bølling section.

7. Discussion and Conclusions

The GICC05 time scale across the last termination (7,903 – 14,776 b2k) has been constructed by identifying and counting annual layers using multi-parameter data sets from the GRIP and NGRIP ice cores. The ages of the onset and end of the Younger Dryas, Bølling and Allerød periods can be found in Table 4 along with the ages of the Saksunarvatn and Vedde volcanic ash layers. In Figure 10, 20 year mean values of NGRIP $\delta^{18}\text{O}$ data are shown on the GICC05 time scale. For comparison, the same $\delta^{18}\text{O}$ data are shown on the previously used time scales: the existing counted time scale for the Holocene part and the ss09sea model time scale below the YDPB transition [Johnsen et al., 1992; 2001]. The GRIP isotope profile is not displayed, as the ss09sea time scale is common to the GRIP and NGRIP cores [NGRIP members, 2004]. The 20 year resolution GISP2 isotope profile of Grootes and Stuiver [1997] and Stuiver and Grootes [2000] is presented on the time scale of Meese et al. [1997]. The differences between the time scales are apparent in Figure 11, where the differences in the dating of 46 selected ECM horizons in the three time scales are shown. At the datum of the GICC05 time scale (8236 b2k), the existing NGRIP time scales yield ages that are about 20 years younger than the GICC05, but the difference grows increasingly fast towards the YDPB transition. The transition has

been dated to 11,703 b2k with a maximum counting error of 99 years, pushing the YDPB transition about 150 years back relative to the previous GRIP and NGRIP age estimates. The difference increases slowly to about 180 years at 12.5 ka b2k, and then monotonically decreases again through the Allerød and Bølling periods until the onset of Bølling, where the difference has been reduced to about 50 years. The differences between the former and new time scales in the Holocene part reflect the new interpretation of the GRIP data, while the differences below the YDPB transition indicate that the relationship between $\delta^{18}\text{O}$ and accumulation used to construct the model time scales [Johnsen et al., 1995; Dahl-Jensen et al., 1993; Johnsen et al., 2001] needs improvement in the Bølling and Allerød periods.

In general, the GICC05 time scale agrees better with the GISP2 time scale than the former GRIP and NGRIP time scales. At the 8.2 ka event the GISP2 time scale yields dates that are 36 years older than the corresponding GICC05 ages, but the main difference between the GICC05 and GISP2 time scales in the Holocene is the number of annual layers in the 8.2–9.5 ka b2k section, where the GISP2 time scale lacks about 60 years, or 5%, relative to the GICC05. It should be noted that the investigators producing the GISP2 time scale did not agree on the number of years in the GISP2 1371 – 1519 m depth interval (GISP2 age 8070 - 9424 b2k), where R.B. Alley counted 72 years more than the number of years in the official GISP2 time scale after the ice core had been stored for a few years [Alley et al., 1997, Table 2]. The GICC05 and GISP2 time scales have roughly the same number of years in the 9.5–11.5 ka b2k section, and agree within a few years on the age of the YDPB transition when the transition depth is defined using deuterium excess data [T. Popp, pers. comm., 2005]. However, the difference grows rapidly in the Younger Dryas section. In the 11.5–12.9 ka b2k section, corresponding to the Younger Dryas and the first 2 centuries of the Preboreal, the GISP2 time scale contains 84 years, or 6%, more years than the GICC05. In the Allerød the two scales agree fairly well again, while GISP2 has about 40, or 6%, years less in the Bølling period relative to the GICC05. Significant differences which cannot be attributed to counting uncertainty thus remain between the GICC05 and GISP2 time scales.

As previously mentioned, the GICC05 time scale has not been transferred to the GRIP depth scale on a year-to-year basis below the YDPB transition due to marginal data resolution, but common features in the ECM signal allow for matching of the two cores. Interpolation is used between fix points, leading to an estimated maximum matching error of 5 years. Björck et al. [1998] defines the Younger Dryas as the GRIP depth interval 1623.6 – 1661.5 m and gives the duration as 1150 ± 50 years. The matching of the GRIP and NGRIP ECM records makes it possible to identify the corresponding depth interval in the NGRIP core, and according

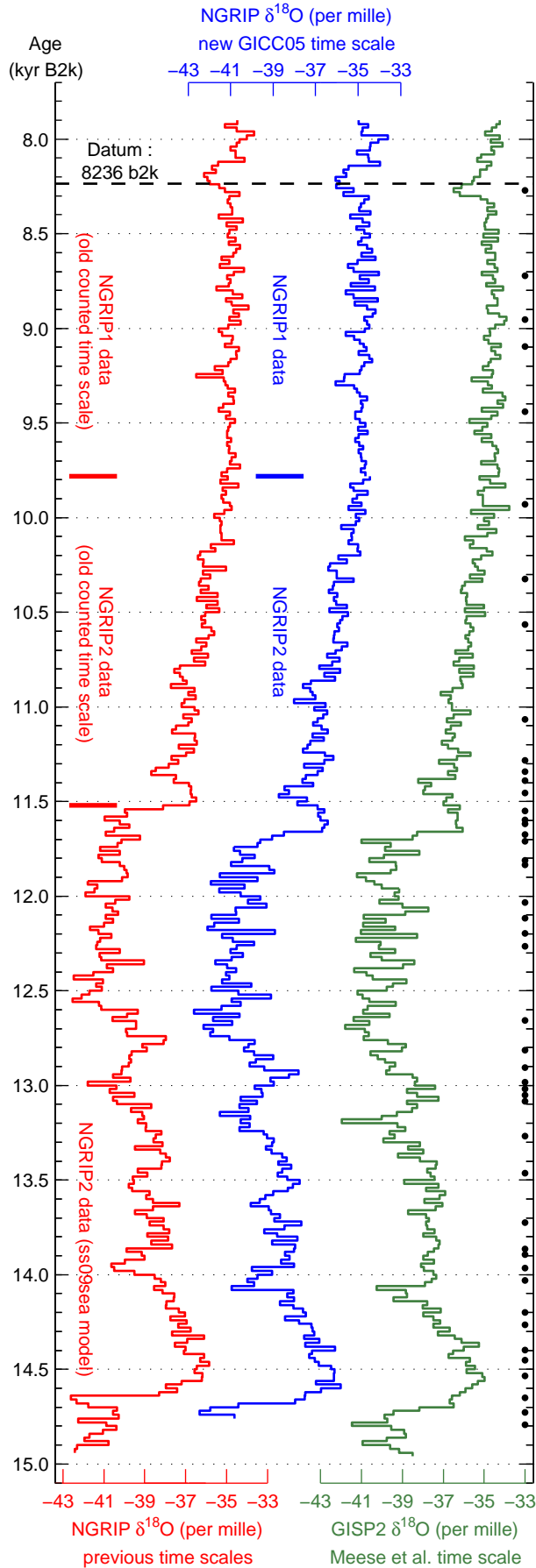


Figure 10. caption in next column

Figure 10. Stable isotope profiles from NGRIP and GISP2 of the entire sections covered by the presented time scale. The red curve shows 20 year mean values of NGRIP $\delta^{18}\text{O}$ data on the existing counted time scale (Holocene part) and ss09sea model time scale (glacial part). The blue curve shows the same data on the new GICC05 time scale. The difference between the shape of the blue and red curves is a consequence of different 20 year averaging intervals, as the underlying $\delta^{18}\text{O}$ data are the same. The green curve show GISP2 $\delta^{18}\text{O}$ data on the time scale of Meese et al. [1997]. The black bullets to the right are the fix points used for the comparison in Figure 11, shown relative to the GISP2 curve.

to GICC05 the duration of the Younger Dryas is evaluated to be 1186 years (maximum counting error 44 years). The deviation from the duration given in Table 3 arises from the different definitions of onset and end depths. The GICC05 timescale thus agrees well with the INTIMATE duration estimate of Björck et al. [1998], even though the onset and termination of the Younger Dryas are 150-200 years older according to GICC05. In the same way, the total duration of the Bølling – Allerød period (GIS-1a through 1e) is given as 2050 ± 50 years by Björck et al. [1998] (GRIP depth 1661.5 – 1753.4 m), while the corresponding duration is only 1818 (maximum counting error 53 years) according to the GICC05 time scale. The combination of the Bølling – Allerød being 200-250 years shorter and the YDPB transition being 150 years older in the GICC05 compared to Björck et al. [1998], means that the age of $14,750 \pm 50$ b2k for the onset of Bølling given by Björck et al. [1998] agrees fairly well with the GICC05 age of 14,692 b2k (maximum counting error 186 years).

It should be emphasized that the maximum counting errors given here reflect a conservative estimate of the maximum error associated with interpretation of ambiguous features in the data, data gaps, and marginal resolution in accordance with the discussion in section 5.1.4, but does not include uncertainty contributions from possible bias in the annual layer identification process, that can not be quantitatively assessed without independent data.

The relative phasing of the different impurity data series is observed to be different during cold and warm conditions, indicating that the annual distribution of precipitation changes rapidly both at the climate transitions and within the Bølling and Allerød periods. The annual layer thicknesses are observed to be log-normally distributed with good approximation, and the ratios of the mean accumulation rates of Younger Dryas and Bølling to that of the Early Holocene are $47 \pm 2\%$ and $88 \pm 2\%$, respectively.

The work with the new Greenland Ice Core Chronology continues, and the time scale presented here will be both extended further back in time and compared and validated by comparison with results from independent dating strategies. Only by providing the ice cores with reliable time scales, the full value of the records extracted from the ice cores can be appreciated and used in conjunction with other palaeoclimatic data, thereby assessing essential questions about the timing of past climatic changes.

8. Online data access

20 year mean values of GRIP and NGRIP $\delta^{18}\text{O}$ data on the GICC05 time scale (as shown for NGRIP in Figure 10) can be downloaded from <http://www.icecores.dk>.

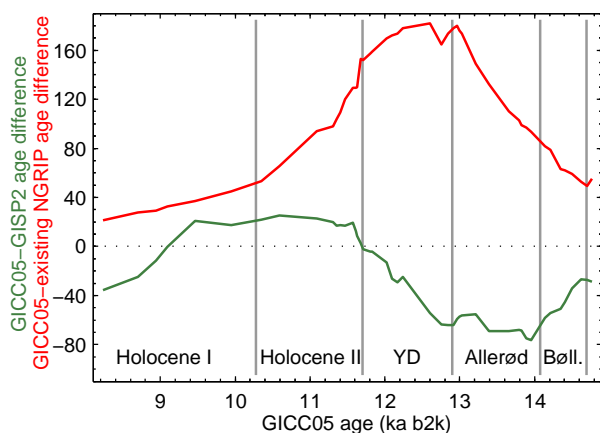


Figure 11. Detailed comparison of the GICC05 time scale with the existing NGRIP/GRIP time scales (specified in the caption of Figure 10) and the GISP2 time scale of Meese et al. [1997] using the dates of 46 common ECM events in the NGRIP, GRIP, and GISP2 cores (see Figure 10). Positive values indicate that an event is oldest according to the GICC05 time scale.

Acknowledgments. This work is a contribution of the Copenhagen Ice Core Dating Initiative which is supported by a grant from the Carlsberg Foundation.

NGRIP is directed and organized by the Ice and Climate Research Group at the Niels Bohr Institute, University of Copenhagen, Denmark. It is supported by funding agencies in Denmark (SNF), Belgium (FNRS-CFB), France (IPEV and INSU/CNRS), Germany (AWI), Iceland (Rannls), Japan (MEXT), Sweden (SPRS), Switzerland (SNF) and the USA (NSF, Office of Polar Programs). SOR gratefully acknowledges Robert Mulvaney, and British Antarctic Survey, for support during a visit to BAS from August to October 2004.

We thank Eric Wolff for comments during review that greatly improved the quality of the uncertainty discussion.

References

- Alley, R., et al. (1993), Abrupt increase in Greenland snow accumulation at the end of the Younger Dryas event, *Nature*, 362(6420), 527–529.
- Alley, R. B., et al. (1997), Visual-stratigraphic dating of the GISP2 ice core: Basic, reproducibility, and application, *Journal of Geophysical Research*, 102(C12), 26,367–26,381.
- Anklin, M., R. C. Bales, E. Mosley-Thompson, and K. Steffen (1998), Annual accumulation at two sites in Northwest Greenland during recent centuries, *Journal of Geophysical Research*, 103(D22), 28,775–28,783.
- Beer, J., et al. (1991), Seasonal variations in the concentrations of ^{10}Be , Cl^- , NO_3^- , SO_4^{2-} , H_2O_2 , ^{210}Pb , ^3H , mineral dust, and $\delta^{18}\text{O}$ in Greenland snow, *Atmospheric Environment*, 25(19), 899–904.
- Bigler, M. (2004), Hochaufösende Spurenstoffmessungen an polaren Eisbohrkernen: Glaziochemische und klimatische Prozessstudien, Ph.D. dissertation, University of Bern, Switzerland.
- Björck, S., M. J. C. Walker, L. C. Cwynar, S. Johnsen, K.-L. Knudsen, J. J. Lowe, B. Wohlfarth, and INTIMATE Members (1998), An event stratigraphy for the Last Termination in the North Atlantic region based on the Greenland ice-core record: a proposal by the INTIMATE group, *Journal of Quaternary Science*, 13(4), 283–292.
- Blunier, T., et al. (1998), Asynchrony of Antarctic and Greenland climate change during the last glacial period, *Nature*, 394, 739–743.
- Bond, G., W. Broecker, S. Johnsen, J. McManus, L. Labeyrie, J. Jouzel, and G. Bonani (1993), Correlations between climate records from North Atlantic sediments and Greenland ice, *Nature*, 365(6442), 143–147.
- Bory, A.-M., P. Biscaye, A. Svensson, and F. Grousset (2002), Seasonal variability in the origin of recent atmospheric mineral dust at NorthGRIP, Greenland, *Earth and Planetary Science Letters*, 196, 123–134.
- Clausen, H., C. Hammer, C. Hvidberg, D. Dahl-Jensen, J. Steffensen, J. Kipfstuhl, and M. Legrand (1997), A comparison of the volcanic records over the past 4000 years from the Greenland Ice Core Project and Dye3 Greenland ice cores, *Journal of Geophysical Research*, 102(C12), 26,707–26,723.
- Cuffey, K., and G. Clow. (1997), Temperature, accumulation, and ice sheet elevation in central Greenland through the last deglacial transition, *Journal of Geophysical Research*, 102, 26,383–26,396.
- Dahl-Jensen, D., S. J. Johnsen, C. U. Hammer, H. B. Clausen, and J. Jouzel (1993), Past accumulation rates derived from observed annual layers in the GRIP ice core from Summit, Central Greenland, in *Ice in the Climate System*, NATO ASI Ser. I, vol. 12, edited by R. W. Peltier, pp. 517–532, Springer-Verlag, New York.
- Dahl-Jensen, D., N. S. Gundestrup, H. Miller, O. Watanabe, S. J. Johnsen, J. P. Steffensen, H. B. Clausen, A. Svensson, and L. B. Larsen (2002), The NorthGRIP deep drilling programme, *Annals of Glaciology*, 35, 1–4.
- Dansgaard, W., et al. (1993), Evidence for general instability of past climate from a 250-kyr ice-core record, *Nature*, 364(6434), 218–220.
- Fischer, H., and D. Wagenbach (1996), Large-scale spatial trends in recent firn chemistry along an east-west transect through central Greenland, *Atmospheric Environment*, 30(19), 3227–3238.
- Fisher, D., R. Koerner, W. Paterson, W. Dansgaard, N. Gundestrup, and N. Reeh (1983), Effect of wind scouring on climate records from ice-core oxygen-isotope profiles, *Nature*, 301, 205–209.
- Fuhrer, K., A. Neftel, M. Anklin, and V. Maggi (1993), Continuous measurements of hydrogen peroxide, formaldehyde, calcium and ammonium concentrations along the new GRIP ice core from Summit, Central Greenland, *Atmospheric Environment*, 27A(12), 1873–1880.
- Fuhrer, K., A. Neftel, M. Anklin, T. Staffelbach, and M. Legrand (1996), High-resolution ammonium ice core record covering a complete glacial-interglacial cycle, *Journal of Geophysical Research*, 101(D2), 4147–4164.
- Fuhrer, K., E. W. Wolff, and S. J. Johnsen (1999), Timescales for dust variability in the Greenland Ice Core Project (GRIP) ice core in the last 100,000 years, *Journal of Geophysical Research*, 104(D24), 31,043–31,052.
- Groote, P. M., and M. Stuiver (1997), Oxygen 18/16 variability in Greenland snow and ice with 10^{-3} to 10^5 -year time resolution, *Journal of Geophysical Research*, 102, 26,455–26,470.
- Hammer, C. (1989), Dating by physical and chemical seasonal variations and reference horizons, in *Dahlem Konferenz: The Environmental Record in Glaciers and Ice Sheets*, edited by H. Oeschger and J. Langway, C.C., Physical, Chemical, and Earth Sciences Research Report 8, pp. 99–121, John Wiley, New York.
- Hammer, C. U., H. B. Clausen, W. Dansgaard, N. Gundestrup, S. J. Johnsen, and N. Reeh (1978), Dating of Greenland ice cores by flow models, isotopes, volcanic debris, and continental dust, *Journal of Glaciology*, 20(82), 3–26.
- Hammer, C. U., H. B. Clausen, and H. Tauber (1986), Ice-core dating of the Pleistocene/Holocene boundary applied to a calibration of the ^{14}C time scale, *Radiocarbon*, 28, 284–291.
- Hammer, C. U., H. B. Clausen, and C. C. Langway, Jr. (1994), Electrical conductivity method (ECM) stratigraphic dating of the Byrd Station ice core, Antarctica, *Annals of Glaciology*, 20, 115–120.

- Hvidberg, C. S., J. P. Steffensen, H. B. Clausen, H. Shoji, and J. Kipfstuhl (2002), The NorthGRIP ice-core logging procedure: description and evaluation, *Annals of Glaciology*, *35*, 5–8.
- Johnsen, S., D. Dahl-Jensen, W. Dansgaard, and N. Gundestrup (1995), Greenland palaeotemperatures derived from GRIP bore hole temperature and ice core isotope profiles, *Tellus*, *47B*, 624–629.
- Johnsen, S. J. (1977), Stable isotope homogenization of polar firn and ice, in *Proc. of Symp. on Isotopes and Impurities in Snow and Ice, I.U.G.G. XVI, General Assembly, Grenoble Aug./Sept., 1975*, pp. 210–219, IAHS-AISH Publ. 118, Washington D.C.
- Johnsen, S. J., W. Dansgaard, and J. White (1989), The origin of Arctic precipitation under present and glacial conditions, *Tellus*, *41B*, 452–468.
- Johnsen, S. J., H. B. Clausen, K. M. Cuffey, G. Hoffmann, J. Schwander, and T. Creyts (2000), Diffusion of stable isotopes in polar firn and ice: The isotope effect in firn diffusion, in *Physics of Ice Core Records*, edited by T. Hondoh, pp. 121–140, Hokkaido University Press, Sapporo.
- Johnsen, S. J., D. Dahl-Jensen, N. Gundestrup, J. P. Steffensen, H. B. Clausen, H. Miller, V. Masson-Delmotte, A. E. Sveinbjörnsdóttir, and J. White (2001), Oxygen isotope and palaeotemperature records from six Greenland ice-core stations: Camp Century, Dye-3, GRIP, GISP2, Renland and NorthGRIP, *J. Quat. Sci.*, *16*, B01402, doi:10.1029/2003JB002550.
- Johnsen, S. J., et al. (1992), Irregular glacial interstadials recorded in a new Greenland ice core, *Nature*, *359*, 311–313.
- Jouzel, J., and L. Merlivat (1984), Deuterium and oxygen-18 in precipitation: Modeling of the isotopic effects during snow formation, *Journal of Geophysical Research*, *89*(D7), 11,749–11,757.
- Laj, P., J. M. Palais, and H. Sigurdsson (1992), Changing sources of impurities to the Greenland ice sheet over the last 250 years, *Atmospheric Environment*, *26A*(14), 2627–2640.
- Langway, Jr., C. C. (1967), Stratigraphic analysis of a deep ice core from Greenland, *CRREL Research Report 77*, pp. 1–130.
- Masson-Delmotte, V., J. Jouzel, A. Landais, M. Stievenard, S. J. Johnsen, J. W. C. White, M. Werner, A. Sveinbjörnsdóttir, and K. Fuhrer (2005a), GRIP deuterium excess reveals rapid and orbital-scale changes in Greenland moisture origin, *Science*, *209*, 118–121, doi:10.1126/science.1108575.
- Masson-Delmotte, V., et al. (2005b), Holocene climatic changes in Greenland: Different deuterium excess signals at Greenland Ice Core Project (GRIP) and NorthGRIP, *Journal of Geophysical Research*, *110*, doi:10.1029/2004JD005575.
- Meese, D. A., A. J. Gow, R. B. Alley, G. A. Zielinski, P. M. Grootes, M. Ram, K. C. Taylor, P. A. Mayewski, and J. F. Bolzan (1997), The Greenland Ice Sheet Project 2 depth-age scale: Methods and results, *Journal of Geophysical Research*, *102*(C12), 26,411–26,423.
- North Greenland Ice Core Project members (2004), High-resolution record of Northern Hemisphere climate extending into the last interglacial period, *Nature*, *431*, 147–151.
- Rasmussen, S. O., K. K. Andersen, S. J. Johnsen, M. Bigler, and T. McCormack (2005), Deconvolution-based resolution enhancement of chemical ice core records obtained by Continuous Flow Analysis, *Journal of Geophysical Research*, *110*(D17304), doi:10.1029/2004JD005717.
- Röthlisberger, R., M. Bigler, M. Hutterli, S. Sommer, B. Stauffer, H. Junghans, and D. Wagenbach (2000), Technique for continuous high-resolution analysis of trace substances in firn and ice cores, *Environmental Science and Technology*, *34*(2), 338–342.
- Ruth, U., D. Wagenbach, J. Steffensen, and M. Bigler (2003), Continuous record of microparticle concentration and size distribution in the central Greenland NGRIP ice core during the last glacial period, *Journal of Geophysical Research*, *108*, 4098, doi:10.1029/2002JD002376.
- Seierstad, I. K., S. J. Johnsen, B. M. Vinther, and J. Olsen (2006), The duration of the Bølling-Allerød period (Greenland Interstadial 1) in the GRIP ice core, *Annals of Glaciology*, in press.
- Southon, J. (2004), A radiocarbon perspective on Greenland ice-core chronologies: Can we use ice cores for ^{14}C calibration?, *Radiocarbon*, *46*(3), 1239–1260.
- Steffensen, J. P. (1988), Analysis of the seasonal variation in dust, Cl^- , NO_3^- , and SO_4^{2-} in two Central Greenland firn cores, *Annals of Glaciology*, *10*, 171–177.
- Stuiver, M., and P. M. Grootes (2000), GISP2 Oxygen isotope ratios, *Quaternary Research*, *53*, 277–284, doi:10.1006/qres.2000.2127.
- Svensson, A., S. W. Nielsen, S. Kipfstuhl, S. J. Johnsen, J. P. Steffensen, M. Bigler, U. Ruth, and R. Röthlisberger (2005), Visual stratigraphy of the North Greenland Ice Core Project (NorthGRIP) ice core during the last glacial period, *Journal of Geophysical Research*, *110*(D2), doi:10.1029/2004JD005134.
- Taylor, K., et al. (1997), The Holocene-Younger Dryas transition recorded at Summit, Greenland, *Science*, *278*, 825–827.
- Vinther, B. M., et al. (2006), A synchronized dating of three Greenland ice cores throughout the Holocene, *Journal of Geophysical Research*, in press, doi:10.1029/2005JD006921.
- Werner, M., U. Mikolajewicz, M. Heimann, and G. Hoffmann (2000), Borehole versus isotope temperatures on Greenland: Seasonality does matter, *Geophysical Research Letters*, *27*(5), 723–726.
- Whitlow, S., P. A. Mayewski, and J. E. Dibb (1992), A comparison of major chemical species seasonal concentration and accumulation at the South Pole and Summit, Greenland, *Atmospheric Environment*, *26A*(11), 2045–2054.

Sune Olander Rasmussen, Ice and Climate, Niels Bohr Institute, University of Copenhagen, Juliane Maries Vej 30, DK-2100 Copenhagen, Denmark. (olander@gfy.ku.dk)